Proceedings of the 2006 IEEE International Conference on Robotics and Automation
Orlando, Florida - May 2006

Dynamic Regrasping Using a High-speed Multifingered Hand and a High-speed Vision System

Noriatsu Furukawa Akio Namiki Senoo Taku Masatoshi Ishikawa
Department of Creative Informatics,
Graduate School of Information Science and Technology,
The University of Tokyo.
7-3-1 Hongo, Bunkyo-ku, Tokyo 113-8656, Japan
Email: noriatsu@k2.t.u-tokyo.ac.jp, Akio_Namiki@ipc.i.u-tokyo.ac.jp, Masatoshi_Ishikawa@ipc.i.u-tokyo.ac.jp

***Abstract*— In most previous studies, it has been difficult for a robot hand to regrasp a target quickly because its motion was static or quasi-static, in a constant contact state. In order to achieve high-speed regrasping, we propose a new strategy which we call dynamic regrasping. In this strategy, the regrasping task is achieved by throwing a target up and by catching it.**

In this paper, a regrasping strategy based on visual feedback is presented and experimental results using a high-speed multi-fingered robot hand and a high-speed vision system are shown. A cylinder is chosen as a specific example of target for dynamic regrasping, with which successful dynamic regrasping tasks are experimentally achieved.

I. Introduction

The need for dexterous robot hands in the industrial and household field is increasing every day and one of the most important functions of such a hand is regrasping. That is to change a grasping state in order to achieve desired tasks.

Several studies on regrasping have been published previously [1]-[5], but several problems have not been encountered. First, robot hands must have many fingers in order to change their grasping states while keeping a stable state. Second, their motion is static or quasi-static, maintaining a state of constant contact and it is not fast.

On the other hand, in the concept of dynamic manipulation, a robot gives acceleration to a target and performs dynamic tasks [6]. In dynamic manipulation, the robot's motion is dynamic and quick and there is no constant contact state.

Using this background, we apply the concept of dynamic manipulation to propose a new strategy which is called "dynamic regrasping." The concept is shown in Fig. 1. In dynamic regrasping, the robot hand throws a target vertically up once to rotate the target and to change its orientation, and catches it when it falls. Dynamic regrasping has three advantages. The first one is the ability to regrasp a target quickly. The second one is that only two manipulations are needed: throwing and catching. The last one is that only a few fingers are needed: three fingers in this study.

In this paper, a regrasping strategy based on visual feedback is presented and experimental results using a high-speed multifingered robot hand and a high-speed vision system are shown.

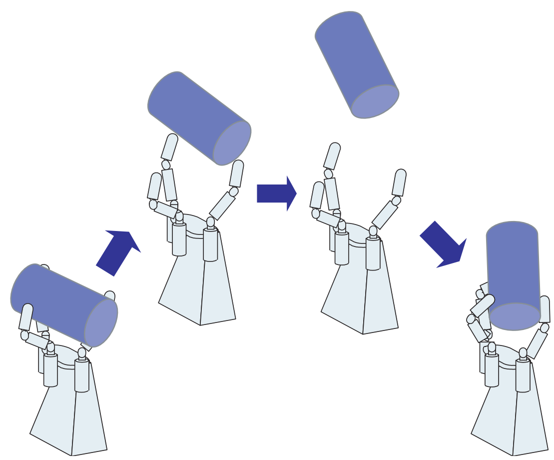

Fig. 1. A concept of dynamic regrasping.

II. Previous Works

Some researchers have worked on regrasping using various types of robot hands. T. Schlegl et al. proposed an approach based on a real-time grasping force optimization algorithm and a fingertip impedance control scheme [1]. M. Kaneko et al. defined a human grasp pattern according to the scale and proposed five basic grasping strategies which are easily applicable for general multifingered robot hands [2]. H. Terasaki et al. focused on motion planning of a manipulator equipped with a parallel two-fingered gripper to execute a primitive task, i.e., moving an object to target position [3]. Y. Hasegawa et al. simplified the searching process for regrasping motion in order to apply it in a real time process [4]. T. Schlegl et al. proposed an approach to model a robotic hand as a hybrid discrete-continuous dynamical system [5]. In previous studies, it was assumed that conventional robot hands perform regrasping tasks while keeping in a contact state, and there has been few works on dynamic manipulation.

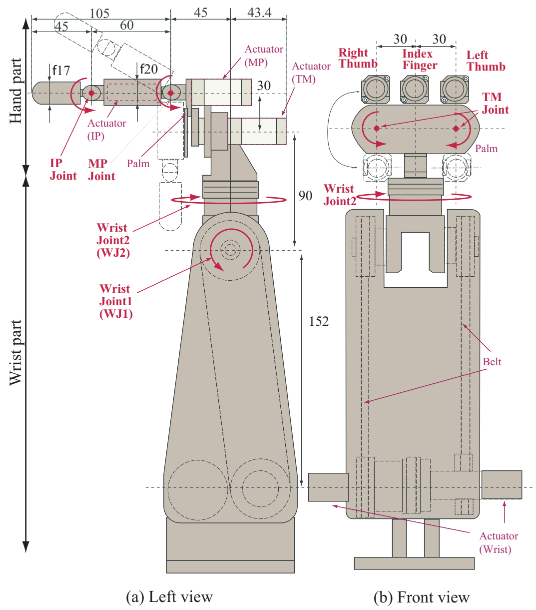

Fig. 2. High-speed multifingered hand.

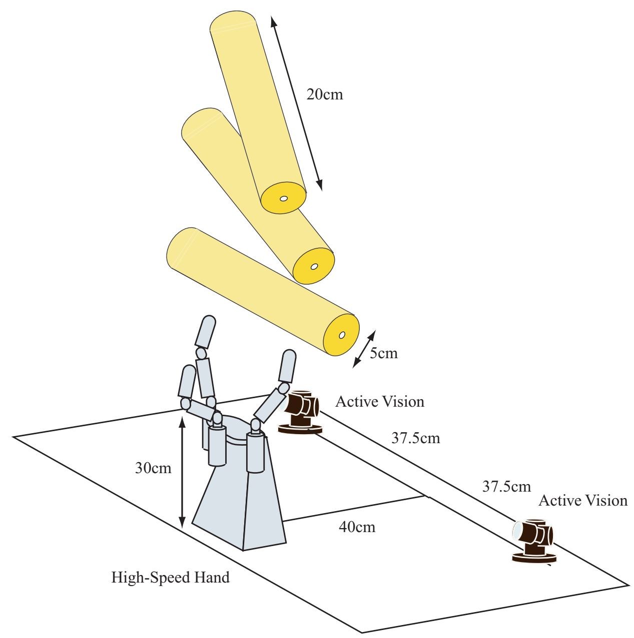

Fig. 3. Experimental system.

M.T. Mason et al. described some preliminary work on dynamic manipulation- some examples, a definition, and analysis of throwing a club [6]. The work on dynamic manipulation has been applied to juggling tasks using a simple manipulator, but not to complicated mechanisms such as a robotic hand, [7].

In order to achieve dynamic fast manipulation, a multifingered hand system with quick finger motion of 180 [deg] in 0.1s has been developed [8]. Using high-speed visual feedback at a rate of 1 [kHz], high-speed catching of a falling ball and a falling cylinder has been achieved [9]. Similar techniques were also applied to high-speed batting [10] and high-speed dribbling [11].

In this study, we achieved regrasping tasks using the high-speed multifingered robot hand based on visual feedback. In contrast to conventional robot hands, the motion of our robot hands is dynamic and quick and uses a non-contact state.

III. System Configuration

In this section, we introduce the experimental system for manipulation by high-speed visual feedback.

A. *High-speed multifingered hand [8]*

Figure 2 shows the mechanical design of the hand. It has three fingers, and we call the fingers “left thumb”, “index finger” and “right thumb” looking from the left side. The index finger has 2-DOF (degrees of freedom), and the other fingers have 3-DOF, so that the hand has 8-DOF in total.

A newly developed small harmonic drive gear and a high-power mini actuator are fitted in each finger link. The design of this actuator is based on the new concept that maximum power output, rather than rated power output, should be improved. The hand can close its joints at 180 [deg] per 0.1 [s].

The hand has two wrist joints. The wrist part has a differential rotation mechanism, and comprises two axes: the flexure-extension axis (WJ1 in Fig. 2) and the abductor-adductor axis (WJ2 in Fig. 2). To minimize the inertia of the hand-wrist unit, actuators are equipped with the root of the elbow, and two belts are used to transmit power from the actuators to the wrist. Its maximum velocity is 300[rpm], and the maximum output is 12[N].

B. *High-speed vision system [8]*

The vision is a massively parallel vision system called CPV-II (column-parallel vision). The CPV-II has 128×128 photo detectors and an all pixel parallel processing array based on the vision chip architecture and an exclusive summation circuit for calculating moment values. Since visual processing is executed in parallel in the processing array, high-speed visual processing (moment detection and segmentation) is achieved, within 1 [ms].

Early image processing in CPV-II is achieved in the following order: segmentation of the image, extraction of the target area, and computation of the image moments. Using two active visions equipped with CPV-II, the 3D position and the 3D orientation of the target are computed. Figure 3 shows the experimental system.

IV. The Strategy of the Dynamic Regrasping

In this section, we describe a strategy of dynamic regrasping. Dynamic regrasping is composed of throwing and catching and both tasks should be achieved precisely. Timing of catching is crucial because the motion is momentary. Thus, a precise and robust strategy is necessary to achieve dynamic regrasping.

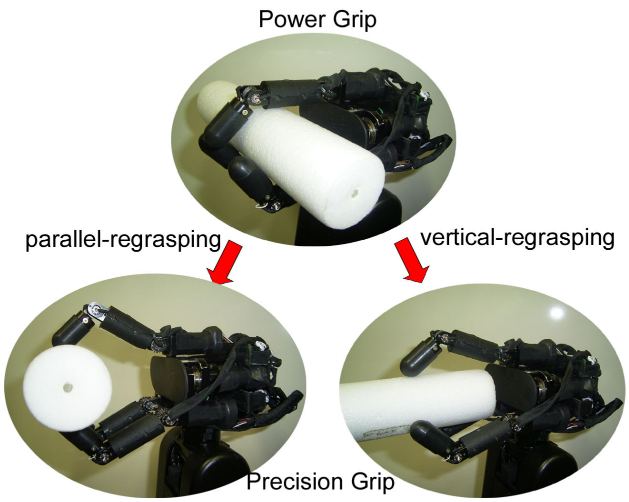

Fig. 4. State transition diagram.

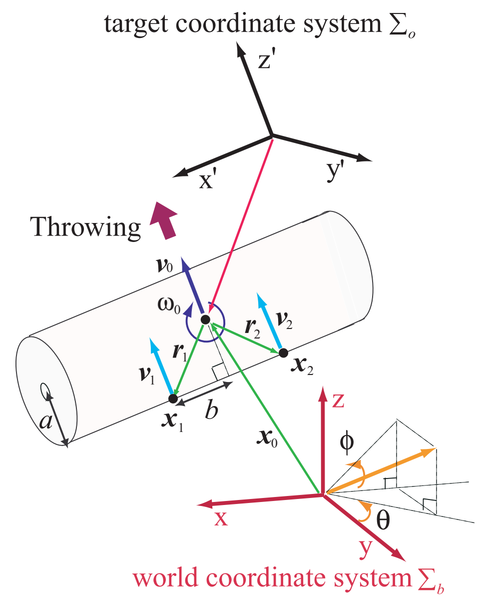

Fig. 5. Coordinate system of a cylinder.

To simplify the problems, we consider a simple target such as a cylinder in a first step of developing dynamic regrasping. Developing and analyzing the strategy with such a target is easier because a cylinder is an axially symmetric object. Figure 4 shows three states of grasping a cylinder by the robot hand. One is a type of power grip, and the others are types of precision grip. In this study, we consider the transitions between two states, from power grip to precision grip as shown in Fig. 4.

We call the case where a robot hand throws a cylinder without changing the orientation of its axis, "parallel-regrasping." The case where a robot hand throws a cylinder so that its axis rotates by 90 [deg], is called "vertical-regrasping."

In order to achieve dynamic regrasping, precise and fast finger and wrist motion is needed together with a system able to track a high-speed target. To meet these requirements, we used the high-speed multifingered hand system and the high-speed vision system described in section III.

In most previous studies, these two state transitions were not achieved quickly because the robot hand had to put the cylinder on the ground once. Thus, these two transitions have been selected to demonstrate the utility of our strategy efficiently.

V. Throwing Strategy

A robot hand must throw a target and rotate it precisely within the range which the robot hand can reach. Therefore, it is important to define a robust throwing strategy.

We divide the throwing phase into two phases in order to analyze this throwing strategy. The first phase is called "before throwing" and the other "after throwing". To simplify the problem, we assume that the target radius and length are given and mass distribution is uniform.

A. before throwing

The position and the orientation of the cylinder have 6-DOF. The cylinder is symmetric with respect to its axis and thus, we can ignore rotation around this axis. In this case, the X-Y-Z coordinate system and $\{\theta\text{-}\phi\}$ is defined in Fig. 5. Σ_o is the coordinate system attached to the cylinder. Σ_b is the world coordinate system.

We determine the three initial conditions in Fig. 6: 1) The Σ_o system is set so that the angle between the z'-axis in Σ_o and the z-axis in Σ_b is α. 2) The velocity given by the fingers is parallel to z'-axis in Σ_o. 3) The cylinder is put statically on the fingers.

The positions of the contact point $\boldsymbol{x}_1$ and $\boldsymbol{x}_2 \in \mathbb{R}^3$ in Σ_b are written as

$$\begin{cases} \boldsymbol{x}_1 = \boldsymbol{x}_0 + R_0 \boldsymbol{r}_1 \\ \boldsymbol{x}_2 = \boldsymbol{x}_0 + R_0 \boldsymbol{r}_2 \end{cases}, \tag{1}$$

where $\boldsymbol{x}_0 \in \mathbb{R}^3$ is the center of gravity of the target, R_0 is the rotation matrix of Σ_o, and $\boldsymbol{r}_1$, $\boldsymbol{r}_2 \in \mathbb{R}^3$ are the relative position of the contact point in the coordinate system of the cylinder.

By differentiating both sides of Eq. (1), we get

$$\begin{cases} \boldsymbol{v}_1 = \boldsymbol{v}_0 + \boldsymbol{\omega}_0 \times R_0 \boldsymbol{r}_1 \\ \boldsymbol{v}_2 = \boldsymbol{v}_0 + \boldsymbol{\omega}_0 \times R_0 \boldsymbol{r}_2 \end{cases}, \tag{2}$$

where $\boldsymbol{\omega}_0 \in \mathbb{R}^3$ is the angular velocity of the target, $\boldsymbol{v}_0 = \dot{\boldsymbol{x}}_0$, $\boldsymbol{v}_1 = \dot{\boldsymbol{x}}_1$, and $\boldsymbol{v}_2 = \dot{\boldsymbol{x}}_2$.

By transferring Eq. (2), we obtain

$$\begin{bmatrix} \boldsymbol{v}_1 \\ \boldsymbol{v}_2 \end{bmatrix} = \begin{bmatrix} I_3 & -R_0 \boldsymbol{r}_1 \times \\ I_3 & -R_0 \boldsymbol{r}_2 \times \end{bmatrix} \begin{bmatrix} \boldsymbol{v}_0 \\ \boldsymbol{\omega}_0 \end{bmatrix}, \tag{3}$$

where $\boldsymbol{r}_1$ and $\boldsymbol{r}_2 \times \in \mathbb{R}^{3\times3}$ is a skew-symmetric matrix associated with a vector $\boldsymbol{r}_1$ and $\boldsymbol{r}_2 \in \mathbb{R}^3$ and I_3 is a unit matrix. By calculating Eq. (3), we derivate

$$\begin{cases} v_{0x} = \dfrac{b}{2a}(v_1 - v_2) \\ \begin{bmatrix} v_{0y} \\ v_{0z} \end{bmatrix} = \begin{bmatrix} \cos\alpha & -\sin\alpha \\ \sin\alpha & \cos\alpha \end{bmatrix} \begin{bmatrix} 0 \\ \dfrac{v_1 + v_2}{2} \end{bmatrix} \end{cases}, \tag{4}$$

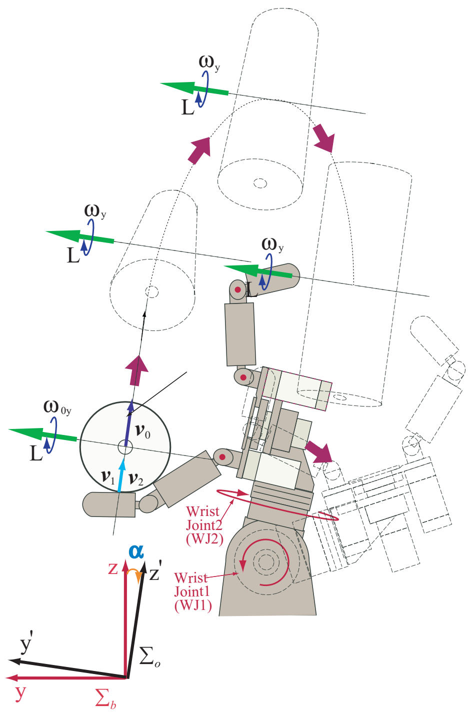

Fig. 6. Throwing phase (Left view).

$$\begin{cases} \omega_{0x} = 0 \\ \begin{bmatrix} \omega_{0y} \\ \omega_{0z} \end{bmatrix} = \begin{bmatrix} \cos\alpha & -\sin\alpha \\ \sin\alpha & \cos\alpha \end{bmatrix} \begin{bmatrix} \frac{1}{2a}(v_1 - v_2) \\ 0 \end{bmatrix} \end{cases}, \tag{5}$$

where $v_1 = \|\boldsymbol{v}_1\|$, $v_2 = \|\boldsymbol{v}_2\|$, v_{0j} and ω_{0j} are the element of $\boldsymbol{v}_0, \boldsymbol{\omega}_0 \in \mathbb{R}^3$ $(j = x, y, z)$, a is the radius of the target, and b is the half distance between x_1 and x_2.

From Eq. (4) and (5), the desired velocity of fingers $\boldsymbol{v}_1$ and $\boldsymbol{v}_2$ are calculated.

B. after throwing

The cylinder is on axial symmetric object, that is, we get $I_{y'} = I_{z'}$ where $I_{x'}$, $I_{y'}$, and $I_{z'}$ are the moment of inertia in the target coordinate system Σ_o. By using Euler's equation, the rotational motion of the cylinder after throwing is written as

$$\begin{cases} I_{x'}\dot{\omega}_{x'} = 0 \\ I_{y'}\dot{\omega}_{y'} - (I_{z'} - I_{x'})\omega_{z'}\omega_{x'} = 0 \\ I_{z'}\dot{\omega}_{z'} - (I_{x'} - I_{y'})\omega_{x'}\omega_{y'} = 0 \end{cases}. \tag{6}$$

Calculating Eq. (4), (5), and (6), we get

$$\begin{cases} \omega_{x'} = 0 \\ \omega_{y'} = \dfrac{1}{2a}(v_1 - v_2) \\ \omega_{z'} = 0 \end{cases}. \tag{7}$$

The angular momentum vector $\boldsymbol{L}_0$ is defined as

$$\boldsymbol{L}_0 = I_{x'}\omega_{x'}^2\boldsymbol{e}_{x'} + I_{y'}\omega_{y'}^2\boldsymbol{e}_{y'} + I_{z'}\omega_{z'}^2\boldsymbol{e}_{z'}, \tag{8}$$

where $\boldsymbol{e}_{i'}(i = x, y, z) \in \mathbb{R}^3$ are unit vectors which gives the principal axes of the target coordinate system Σ_o. From Eq. (8) and the theorem of conservation of angular momentum, we get

$$\boldsymbol{L}_0 = I_{y'}\omega_{y'}^2\boldsymbol{e}_{y'} = \text{const.}. \tag{9}$$

Consequently, $\boldsymbol{L}_0$ has only a component in the $\boldsymbol{e}_{y'}$ direction.

As a result, the target drops keeping its rotation axis at constant orientation. We use the parabolic orbit of the center of the gravity, the hang time, and the initial velocity of the cylinder to calculate the orientation of the target when it falls down.

In this study, we assume that the cylinder is an axially symmetric object. If the cylinder is not axially symmetric object, we have to modify Eq. (7). Then, we get $\omega_{x'}, \omega_{z'} \neq 0$ in Eq. (7). $\boldsymbol{L}_0$ has components in the three $\boldsymbol{e}_{x'}, \boldsymbol{e}_{y'}$, and $\boldsymbol{e}_{z'}$ directions. Thus, the target drops without keeping its rotation axis at constant orientation.

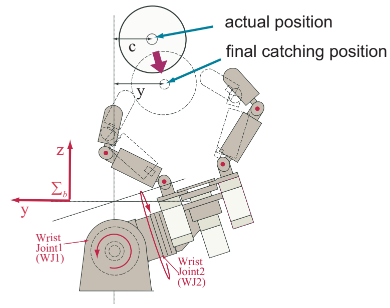

Fig. 7. Catching phase (Control wrist joint 1) (Left view).

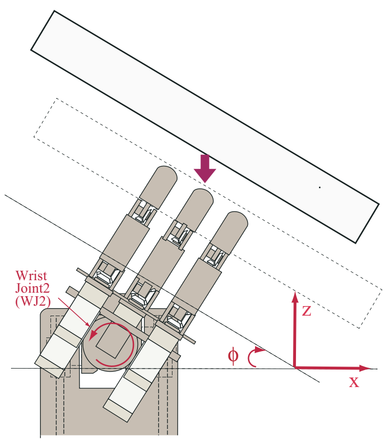

Fig. 8. Catching phase (Control wrist joint 2) (Back view).

VI. Catching Strategy

In this section, we describe the catching strategy. It is difficult to throw a target precisely because various error can occur: in the parameters of the target, in the throwing model, and so on. It is thus necessary to control the robot hand robustly by visual feedback against such errors.

The robot hand uses both parallel-regrasping and vertical-regrasping according to the orientation angle of the cylinder.

A. parallel-regrasping

In this case, the robot hand is controlled in each of the 4-DOF $\{y, z, \theta, \phi\}$ of the cylinder. The robot hand cannot be controlled for changing the x-position, because of its structure.

Changes of the y-position are achieved by controlling the wrist joint 1, as shown in Fig. 7. Concretely, the wrist joint 1 is controlled to meet the condition $c = y$ where c is the y-position of the actual position and y is the y-position of the final catching position. As for the change of the z-position, it is not necessary to control the robot hand because the target falls under the action of the force of gravity. Changes of the ϕ-angle are achieved by controlling the wrist joint 2 to meet the condition that the angle of the target orientation equals the angle of the wrist joint 2, as shown in Fig. 8. Changes of the θ-angle are controlled by the finger joints, as shown in Fig. 9.

We describe now in detailed changes of the θ-angle [9]. Figure 9 shows a simple kinematic model of the movement in the horizontal plane. Let us consider a strategy for manipulating the target from the initial state where the orientation to the final state in the horizontal plane is θ-angle [deg].

Each finger is designated F1, F2, and F3, and it is assumed that the fingers and the target make point contact. First, in order to obtain rotational velocity ω, an impulse force P_1 is given to the target by F1. However, the target takes on not only rotational velocity but also translational velocity. In order to cancel this, it is necessary to give an impulse force P_2 by F2 from the oppsite side simultaneously. Then we obtain

$$\begin{aligned} Mv &= P_1 - P_2, \\ I\omega &= c\cos\theta P_1 + d\cos\theta P_2, \end{aligned} \tag{10}$$

where v is the velocity of center the target, M is the mass of the target, I is the moment of inertia, c and d are the distance from the center of the target to the contact point of F1 and F2 on the main axis respectively. Next, assuming $P_1 \simeq P_2 \equiv P$ and using a geometric condition $c + d = D/\cos\theta + 2R\tan\theta$ (D is the interval between the fingers, R is the radius of the cylinder), we can obtain

$$\begin{aligned} v &= 0, \\ \omega &= (D + 2R\sin\theta)P/I. \end{aligned} \tag{11}$$

We take the center of gravity of the target to correspond to the center of the hand. However, even if they do not correspond, the same result as Eq. (11) is obtained by similar calculations. That is, regardless of the center of gravity, if the values of P_1 and P_2 are equal, a constant angular velocity ω is obtained. Since the rotation center is the center of gravity in this case, however, it is necessary to adjust the center of gravity of the target with respect to the hand center so that the target rotates well on the center of the hand.

B. vertical-regrasping

In this case, the robot hand is controlled in each of the 5 DOF $\{x, y, z, \theta, \phi\}$ of the target. For changes of $\{y, z, \theta\}$, the robot hand is controlled by the same strategy as in parallel-regrasping. Changing the x-position is achieved by controlling the wrist joint 2 as shown in Fig. 8. As for changes of the ϕ-angle, no control is necessary because the target is vertical when it falls.

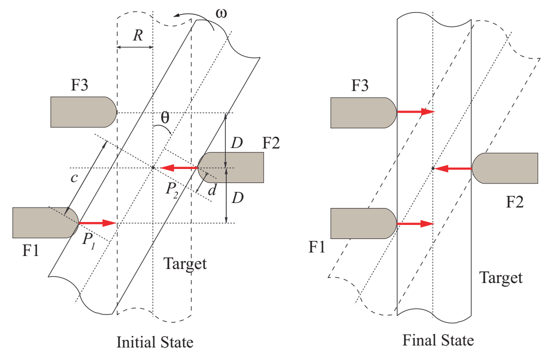

Fig. 9. Catching phase (Control finger joints) (Top view).

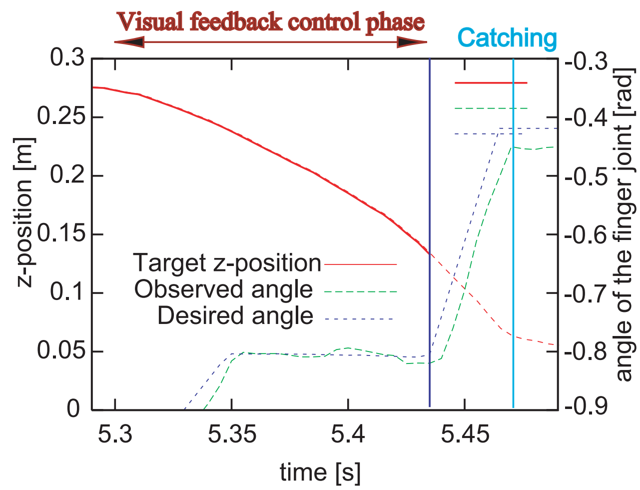

Fig. 10. z-position of the target and angle of the finger joint.

VII. Experiment

A. Experimental setup

We used a styrofoam cylinder, whose diameter was 5 [cm] and length 20 [cm], as the target. We mounted it on a robot hand and the robot hand threw it and caught it. The target position and orientation were computed by the CPV-II system.

B. Experimental result

The experimental result is shown as a movie on the web site [12].

Figure 10, Fig. 11, and Fig. 12 are the results of dynamic regrasping. The y-position and the angle of orientation of the target do not correspond to its actual motion from 5.43 [s] onward. The robot hand is not controlled by visual feedback from 5.43 [s] onward because a part of the target is hidden behind the robot hand.

Figure 10 shows the z-position of the target and the angles of the finger joint. In this experiment, the z-position at which the robot hand should catch the target was 0.07 [m]. The finger

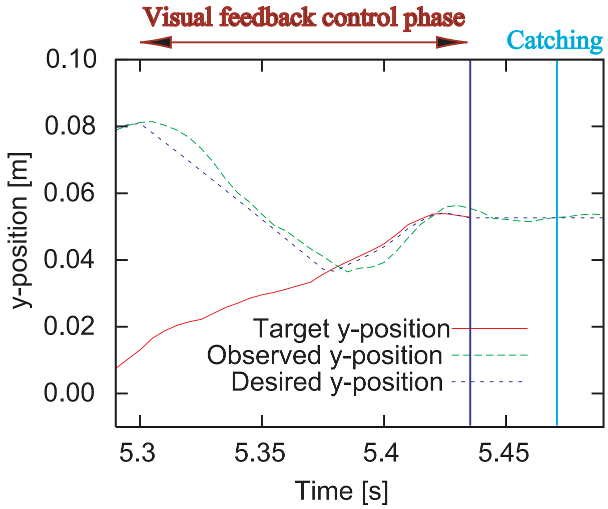

Fig. 11. y-position of the target and y-position of the final catching position.

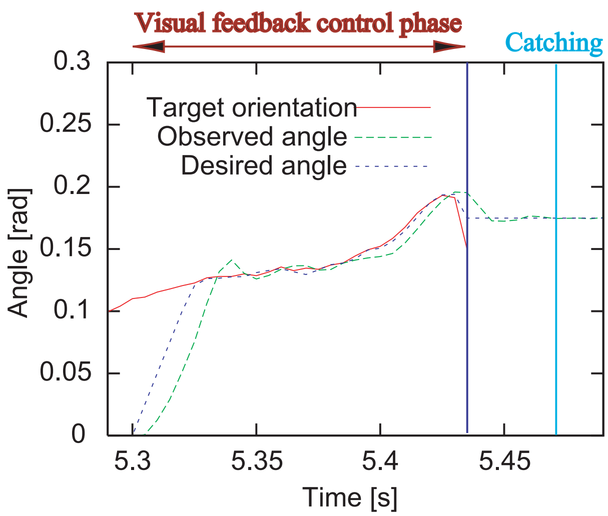

Fig. 12. Angle of the target orientation (ϕ) and angle of the wrist joint 2.

was controlled precisely in response to the z-position of the target and caught the target at 5.47 [s].

Figure 11 shows the y-position of the target and the y-position of the final catching position. The wrist joint 1 was controlled precisely in response to the y-position of the target from 5.3 [s] to 5.43 [s] (Visual feedback control phase).

Figure 12 shows the angle of the target orientation and the wrist joint 2. The wrist joint 2 is controlled precisely in response to the angle of the target orientation from 5.3 [s] to 5.43 [s] (Visual feedback control phase).

Figure 13 and 14 show the experimental results of parallel-regrasping and vertical-regrasping as a continuous sequence of images. The robot hand is throwing a target using its fingers, and each finger and wrist is moving properly in response to the position and orientation of the target, and finally catching is achieved.

The success rate for the experiments was about 35%. The largest cause of the failure is that timing of catching is critical. In the case when the velocity of the cylinder is 2 [m/s], the diameter of the cylinder is 5 [cm], and the diameter of the finger of the hand is 1.8 [cm], the allowable time error is estimated at about ± 0.002 [s]. Thus, it was difficult to calculate the timing for catching accurately.

The other causes of the failure are error on the target and in the model for throwing and catching. We calculated the throwing error and for parallel-regrasping, the y-position error was ± 2 [cm] while for vertical-regrasping, the ϕ-angle error was ± 0.3 [rad]. The cause of the error is mainly an error on the parameters of the target and the existence of a periaxial rotation around the x'-axis and the z'-axis.

VIII. Conclusion

In this paper, we described a new strategy for regrasping and presented experimental results. The dynamic regrasping tasks are achieved using a high-speed multifingered hand and a high-speed vision system. This study is the first step of a more complete analysis of dynamic regrasping. In the future, we will study dynamic regrasping for non-symmetric objects, learning of the unknown parameters by calculating the orientation of the target, and continuous dynamic regrasping, we will be able to enhance the ability of the robot hand phenomenally.

References

[1] T. Schlegl, M. Buss, T. Omata, G. Schmidt. "Fast dexterous re-grasping with optimal contact forces and contact sensor-based impedance control," *Proc. of 2001 IEEE Int. Conf. on Robotics and Automation,* Vol.1, pp. 103-108, 2001.

[2] M. Kaneko T. Shirai, T. Tsuji. "Scale-dependent grasp," *IEEE Transactions on Systems, Man and Cybernetics, Part A (Systems and Humans),* Vol.30(6), pp. 806-816, Nov. 2000.

[3] H. Terasaki, T. Hasegawa. "Motion planning of intelligent manipulation by a parallel two-fingered gripper equipped with a simple rotating mechanism," *Robotics and Automation, IEEE Transactions,* Vol.14(2), pp.207-219, April 1998.

[4] Y. Hasegawa, M. Higashiura, T. Fukuda. "Simplified generation algorithm of regrasping motion - performance comparison online-searching approach with EP-based approach," *Proc. of 2003 IEEE Int. Conf. on Robotics and Automation* Vol.2, pp. 1811-1816, 14-19 Sept. 2003.

[5] T. Schlegl, M. Buss. "Hybrid closed-loop control of robotic hand regrasping," *Proc. of 1998 IEEE Int. Conf. on Robotics and Automation,* Vol.4, pp. 3026 - 3031, 16-20 May 1998.

[6] M .T. Mason and K .M. Lynch. "Dynamic manipulation," *Proc. Int. Conf. Intelligent Robots and Systems,* pp. 152-159, 1993.

[7] A. A. Rizzi and D. E. Koditschek. "Further Progress in Robot Juggling: The Special Two-Juggle," *Proc. of 1993 IEEE Int. Conf. on Robotics and Automation,* pp. 919-924, May 1993.

[8] A. Namiki, Y. Imai, M. Ishikawa, and M. Kaneko. "Development of a High-speed Multifingered Hand System and Its Application to Catching," *Proc. Int. Conf. Intelligent Robots and Systems,* pp. 2666-2671, 2003.

[9] Y. Imai, A. Namiki, K. Hashimoto and M. Ishikawa. "Dynamic Active Catching Using a High-speed Multifingered Hand and a High-speed Vision System," *Proc. of 2004 IEEE Int. Conf. on Robotics and Automation,* pp. 1849-1854, April 2004.

[10] T. Senoo, A. Namiki, and M. Ishikawa. "High-Speed Batting Using a Multi-Jointed Manipulator," *Proc. of 2004 IEEE Int. Conf. on Robotics and Automation,* pp. 1191-1196, 2004.

[11] D. Shiokata, A. Namiki, and M. Ishikawa. "Robot Dribbling Using a High-speed Multifingered Hand and a High-speed Vision System," *Proc. of 2005 IEEE Int. Conf. on Intelligent Robots and Systems,* pp. 3945-3950, 2005.

[12] http://www.k2.t.u-tokyo.ac.jp/fusion/DynamicRegrasping/

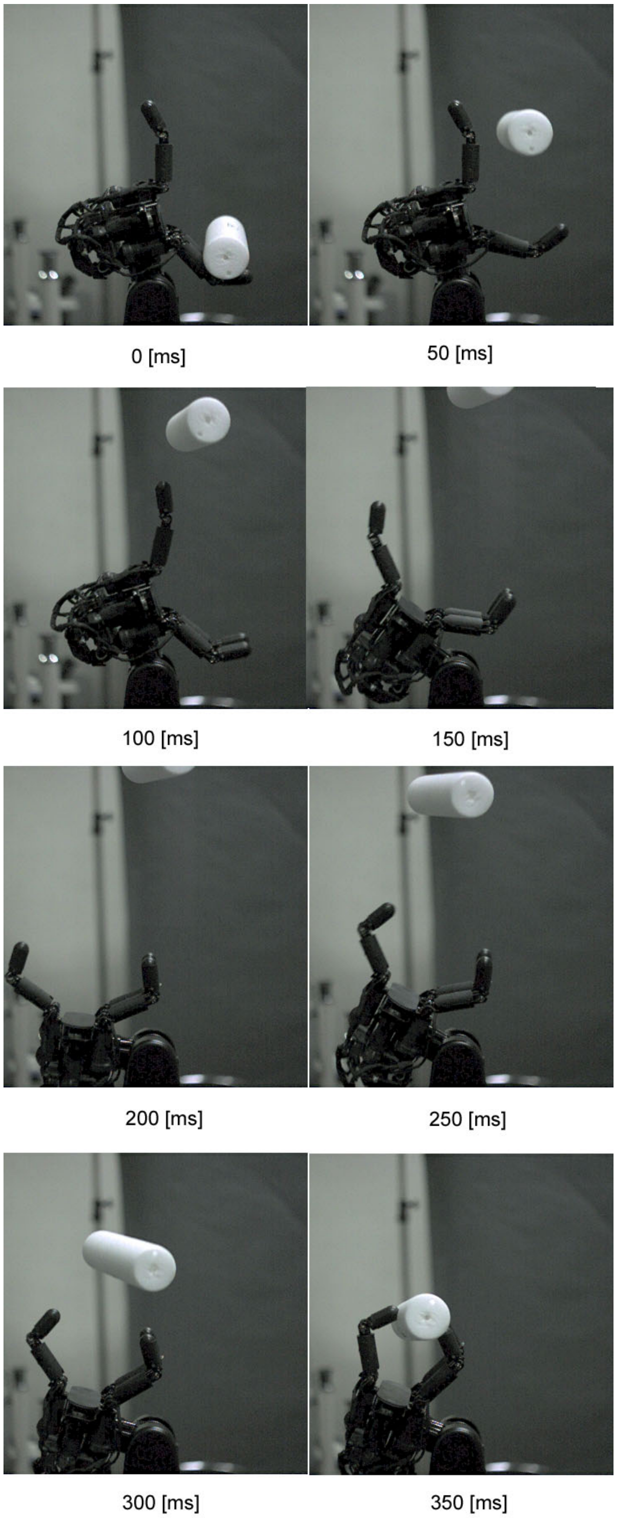

Fig. 13. Experimental result (parallel-regrasping).

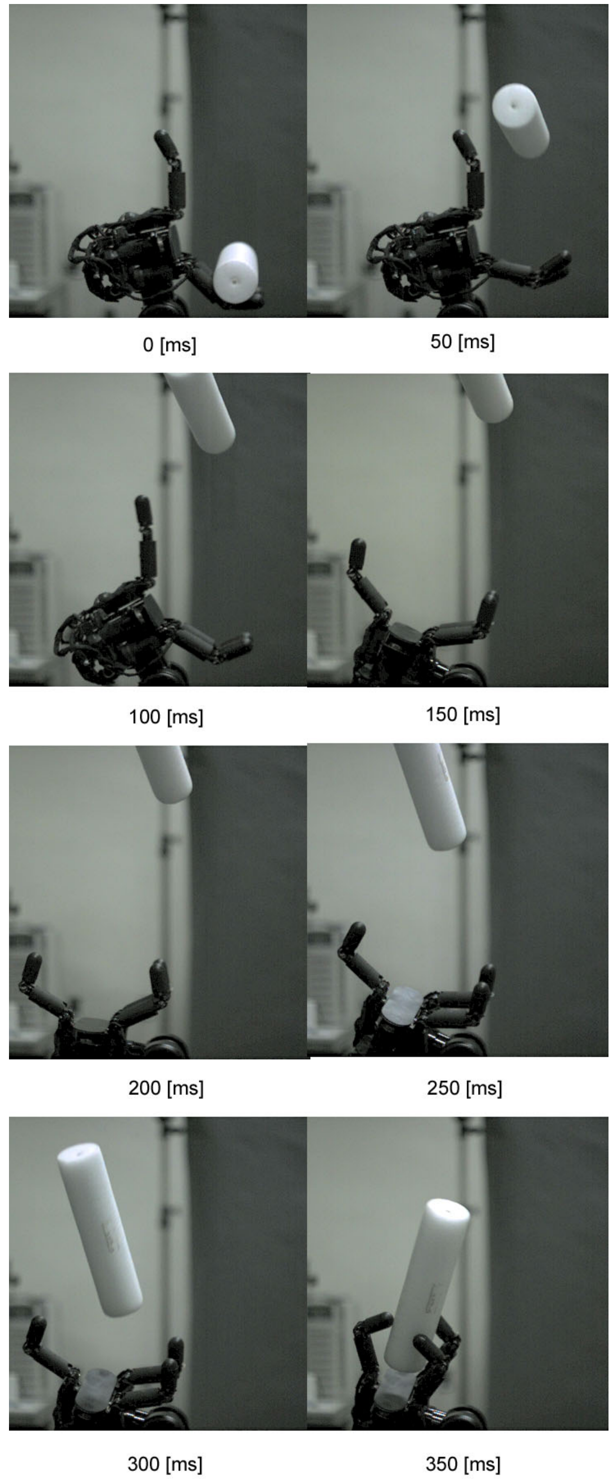

Fig. 14. Experimental result (vertical-regrasping).